How Effectively do Pedestrian Protocol Headform Tests Capture Pedestrian Head Injuries?

Karan S. Devane, Colin Edwards, Luis Poveda, Logan Miller, William Armstrong, Madeline Pollock, Fang-Chi Hsu, F. Scott Gayzik, Ashley A. Weaver, Joel D. Stitzel

Abstract Current pedestrian safety protocols rely on the Head Injury Criterion (HIC_{15}), which often fails to capture rotation-induced brain injuries. This study utilised LS-DYNA to evaluate headform test effectiveness through a large matrix of 1,152 full-body crash simulations. The research utilised 81 generic vehicle models with unique front-end geometry and five human body models (6-year-old, $5^{th}/50^{th}$ percentile females, and $50^{th}/95^{th}$ percentile males) at impact speeds of 30, 40, and 50 km/h. Injury risks (HIC_{15}, BrIC, $CSDM_{25}$) across three scenarios were compared: full-body simulations, headform tests (Euro NCAP protocol), and isolated detailed head-only impacts. HIC_{15}-based injury risk calculated directly within a full-body simulation fails to reflect head injuries, but the headform simulations' HIC_{15}-based injury risk acts as an effective safety proxy. Furthermore, 17.5% of head impacts occurred on the windshield, a critical region for adults currently excluded from proposed FMVSS 228 and GTR 9 standards. Consistent with epidemiological data, the study analysis suggests that Euro NCAP's 40 km/h test speed and four-zone approach (up to WAD 2500) more accurately reflect real-world impacts than FMVSS 228. We conclude that exclusive reliance on HIC_{15} is insufficient for robust protection. Future safety standards should expand testable areas to WAD 2500, including the windshield, and adopt rotation-sensitive metrics like BrIC and $CSDM_{25}$ for virtual testing to capture the full spectrum of brain injury risks.

Keywords Computational model, Headform impact, Head injury, Vulnerable road user, Pedestrian safety.

I. INTRODUCTION

Pedestrian fatalities and severe traumatic brain injuries (TBI) remain a significant challenge for global road safety. In the United States and Europe, regulatory frameworks like European New Car Assessment Programme (Euro NCAP) and the proposed Federal Motor Vehicle Safety Standard (FMVSS) 228 aim to mitigate these injuries by assessing vehicle "aggressiveness" through standardised headform impact tests [1-3]. These protocols rely heavily on the Head Injury Criterion (HIC_{15}), a metric based solely on linear acceleration. However, a growing consensus in biomechanics research suggests that HIC_{15} often fails to predict injuries caused by head rotation, which are primary drivers of TBIs such as diffuse axonal injury and subdural hematoma [4,5].

The effectiveness of current protocols is further limited by their reliance on fixed impact parameters, typically a headform impact velocity of 40 km/h at specific angles. Real-world crash dynamics are far more stochastic. Recent studies utilizing Principal Component Analysis (PCA) on the US vehicle fleet have demonstrated that three primary geometric factors: hood height, hood angle, and hood length, account for over 96% of the variance in vehicle front-end design [6,7]. These geometric variations significantly influence the Head Impact Time (HIT), Head Impact Velocity, and Head Velocity Angle across different pedestrian statures. While surrogate models have shown high accuracy in predicting HIT (R^2 = 0.979) [8], there remains a gap in understanding how these diverse kinematic profiles translate into specific injury risks across a full range of pedestrian sizes and vehicle shapes.

Another critical point of contention is the definition of the "testable zone". While Euro NCAP includes the windshield in its pedestrian protection assessment [9], the proposed FMVSS No. 228 [2] and the international United Nations Global Technical Regulation (UN GTR) No. 9 exclude the windshield from their mandatory headform test areas primarily due to technical practicability, occupant safety concerns, and assessments of injury risk and not due to lower real-world incidence rate. Epidemiological data indicates that the windshield and A-

K. S. Devane is an Assistant Professor (phone: +1 336 716 3260, email: karan.devane@wfusm.edu), C. Edwards is a research engineer, L. Poveda and W. Armstrong are graduate students, L. Miller is a senior research associate, M. Pollock is an undergraduate intern, F. S. Gayzik, A. A. Weaver, and J. D. Stitzel are Professors of Biomedical Engineering in the Center for Injury Biomechanics, FC. Hsu is a Professor at the Department of Biostatistics and Data Science at the Wake Forest University School of Medicine in Winston-Salem, NC, USA.

pillars are leading sources of severe head trauma, particularly for adult pedestrians [10]. Windshield contact is the second most frequent source of serious head injury in both US Pedestrian Crash Data Study data (27% of serious cases) and European German In-Depth Accident Study (GIDAS) data (15%) [11,12]. Excluding the windshield from safety countermeasures reduces protective coverage of severely injured pedestrians from 73% to 44% [12]. Furthermore, organisations such as the IIHS have advocated extending the Wrap Around Distance (WAD) to 2500 mm to better reflect these real-world impact distributions [13]. Without accounting for the high-frequency contact points on the windshield and the variance in impact velocity caused by vehicle geometry, current protocols may provide a narrow and potentially misleading assessment of pedestrian safety.

Computational modeling, specifically high-fidelity Finite Element (FE) analysis, provides a robust method to bridge the gap between fixed-parameter testing and real-world variability. By simulating collisions with Human Body Models (HBMs), researchers can evaluate injury risks like the Brain Injury Criterion (BrIC) and Cumulative Strain Damage Measure ($CSDM_{25}$), which are sensitive to the rotational kinematic components often missed by headform-only tests.

The objective of this study was to perform a comprehensive computational evaluation of pedestrian headform protocol effectiveness. Utilising a database of 1,152 vehicle-to-pedestrian simulations, we assessed 81 generic vehicle (GV) models representing the US fleet and five distinct HBMs ranging from a 6-year-old child to a 95th percentile male. This study specifically analyses the distribution of head impact locations, noting that 17.5% of contacts occur within the windshield region, and evaluates the validity of HIC_{15} against rotation-sensitive metrics across a diverse matrix of impact velocities and angles. This study quantifies the robustness of current and proposed pedestrian safety standards against a high-fidelity, real-world crash matrix of 1,152 successful simulations. The goal of the study was to compare head injuries from full-body simulations which are representative of real-world vehicle-to-pedestrian impacts to the protocol headform tests.

II. METHODS

Baseline Vehicle-to-Pedestrian Crash Simulations

Data from 1,215 vehicle-to-pedestrian crash FE simulations from a design of experiments (DOE) with vehicle front-end geometry, pedestrian size and impact speed as design variables were utilised for this study [7]. The vehicle geometry varied by using 81 GV models representing the US vehicle fleet. The baseline GV models used in the study were updated to include deformable windshield and improved stiffnesses of various front-end parts and are explained in the previous study [7,14]. Updates to the GV models were based on their performance in pedestrian protocol testing simulations. This involved comparing headform, lower legform, and upper legform impacts at various vehicle locations against real-world data from Euro NCAP and NHTSA tests. Five finite element human body models (FEHBMs) of pedestrians representing a 6-year-old child (6YO), 5th (F05) and 50th (F50) percentile females, and 50th (M50) and 95th (M95) percentile males were used to consider variation in pedestrian size. Vehicle-to-pedestrian crash simulations were carried out at three impact speeds based on the Euro NCAP pedestrian protocol CP 540 [15]. The details of the simulation setup are reported by Poveda *et al.* [7]. An example of a full vehicle-to-pedestrian crash simulation setup from this previous study is shown in Fig. 1. For this study, the HIT, location, velocity, angle, WAD and various head injury metrics data were extracted from these full body simulations.

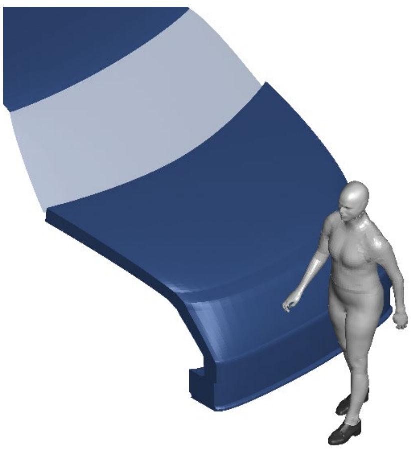

Fig. 1. Simulation setup for vehicle-to-pedestrian crash using F50 model.

Headform and Head-Only Impact Simulations

Using the head impact location from the full body simulations, headform and head-only impact setups were created that followed the Euro NCAP headform impact protocol [1]. The centre of gravity of the headform and head-only models were aligned to make sure they are consistent in all the simulations. Both the adult headform and head-only models were impacted at an angle 65° about the horizontal plane when the impacting location was on the hood and windshield and at 20° when the head impact location was below the hood leading edge height. For the child, these impact angles were 50° and 0°, respectively. Both the headform and head-only models were assigned to an initial velocity of 40 km/h as per the Euro NCAP protocol. All the models used for the headform and head-only model impact simulations, and their mass information are reported in TABLE I. All the head models were extracted from the Global Human Body Models Consortium (GHBMC) detailed occupant models that have deformable parts in the head and are capable of predicting brain injuries. Head masses of these head models were comparable to those of the full pedestrian models. The headform and head-only simulations were carried out only for cases that had head contact with the GV model in the full body simulations.

TABLE I
HEADFORM AND HEAD-ONLY MODEL DETAILS

Subject	Headform (LSTC Models)	Headform Mass (kg)	Head-Only Model	Head-Only Model Mass (kg)
6YO	Child V1.03.2BETA	3.47	Scaled F05	3.37
F05	Adult V4.10.3	4.58	F05	3.52
F50	Adult V4.10.3	4.58	Scaled F05	4.26
M50	Adult V4.10.3	4.58	M50	4.67
M95	Adult V4.10.3	4.58	M95	4.68

Full body baseline head impact from an impact of F50 at 50 km/h and the corresponding headform and head-only impact setups are shown in Fig. 2. Like full body simulations, various head injury metrics were extracted from these simulations which are listed in TABLE II. Brain injury related metrics such as $CSDM_{25}$ were only extracted from the full body and head-only simulations as the headform model lacks instrumentation for those.

(a) (b) (c)

Fig. 2. Simulation setups showing head impact location with full body simulation (a) and corresponding setups for headform impact (b) and head-only impact (c).

TABLE II
LIST OF HEAD INJURY METRICS EXTRACTED FROM THE SIMULATIONS

Full Body	Head-Only	Headform
HIC_{15}	HIC_{15}	HIC_{15}
BrIC	BrIC	BrIC
$CSDM_{25}$	$CSDM_{25}$	-

Analysis

Head injury risk for all three types of simulations was calculated based on the injury metrics listed in TABLE II. The head injury risk was compared between the baseline full-body, headform impact, and head-only impact simulations. The head impact location and WAD from the baseline full body simulations were stratified by different vehicle regions and models, whereas head impact velocity was stratified by impact speed, and head velocity angle by vehicle regions.

III. RESULTS

1,152 simulations from the 1,215 full body DOE simulations had head contact with the GV model and no error terminations, so 1,152 headform and head-only impact simulations were carried out for each. The distribution of head impact location counts for all five models are shown using a heatmap in Fig. 3. Ninety-one head impacts for 6YO and two for F05 were in the bumper area. Only 6YO had two head impacts on the hood leading edge. All models except 6YO had the head impacting the hood, cowl, and windshield. Only one roof head contact was observed for the M95 subject model.

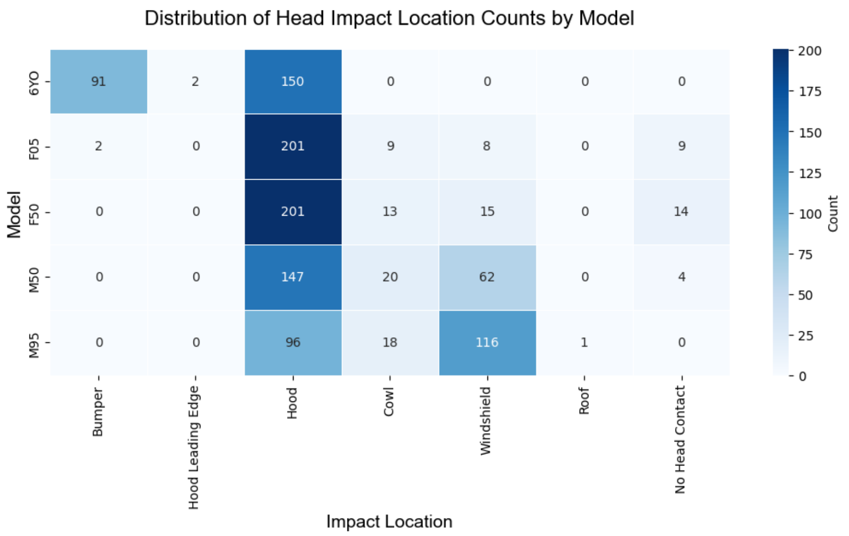

Fig. 3. Distribution of head impact location by model from the baseline full body simulations.

The WAD was stratified by model and impact location to see its distribution within various WAD regions used in pedestrian protocols for headform tests and is shown in Fig. 4 and tabulated in TABLE A1. The shaded gray areas in the background are used for representing WAD regions of 0-1000, 1000-1500, 1500-1700, 1700-2100, 2100-2500, and 2500+ mm. The WAD region 1500-1700 was used to represent the overlap region used by the Euro NCAP pedestrian protocol where tests are conducted using both child and adult headforms. Around 294 adult head contacts were in the 1500-1700 mm WAD overlap region which essentially validates Euro NCAP's dual headform testing strategy.

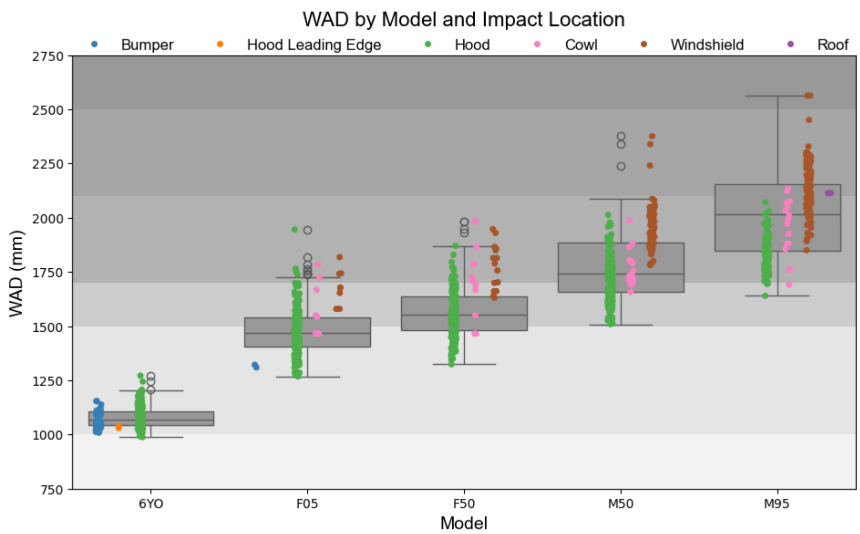

Fig. 4. Distribution of WAD stratified by head impact location from baseline full body simulations overlaid on boxplots for each model. Different colored data points show various head impact locations. Shaded areas in the background are used to show various WAD regions used in the pedestrian protocols.

Having established the spatial distribution of head impacts across the vehicle front end, it is critical to evaluate the kinematic severity of these impacts. The combined analysis of head impact conditions reveals a clear dependence on both pedestrian anthropometry and vehicle impact severity. The scatter plot (Fig. 5a) demonstrates a strong positive correlation between vehicle impact speed and head impact velocity, with the 50 km/h impact speed group consistently producing the highest head impact velocities, often exceeding 50 km/h across the recorded WAD. While head impact velocities generally trend upward with increasing WAD, the 30 km/h impact speed cases largely remain below the 35 km/h head impact velocity threshold. In contrast, the 40 km/h impact speed cases center around the 35–40 km/h head impact velocity range, frequently crossing the 40 km/h threshold as WAD exceeds 1400 mm. The cluster on the left represents data from the 6YO model. The aggregate distribution of these impacts (Fig. 5b) confirms a significant shift toward higher-severity contacts. The histogram shows a multi-modal distribution peaking between 30–35 km/h, with a secondary concentration in the 45–55 km/h range. Quantitatively, a substantial portion of the dataset falls within high-risk zones: 685 cases exceeded the 35 km/h threshold, and 549 cases surpassed the 40 km/h threshold. Together, these data indicate that higher vehicle speeds not only increase the mean head impact velocity but also significantly expand the range of WADs where critical safety thresholds are exceeded.

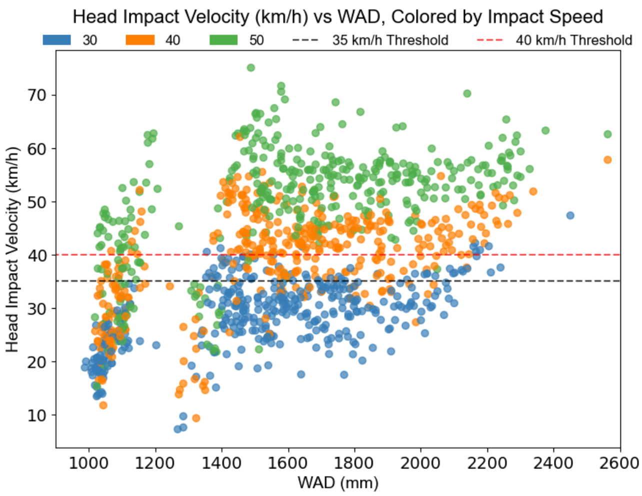

(a)

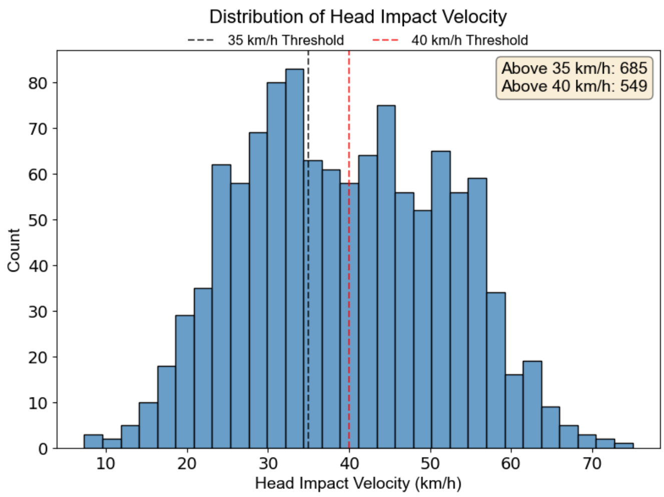

(b)

Fig. 5. Distribution of Head Impact Velocity stratified by impact speed along WAD (a) and histogram of Head Impact Velocity (b). Dashed black and red lines represent headform test velocity used by GTR 9 and Euro NCAP protocols.

Fig. 6 illustrates the variation in head velocity angle relative to WAD, categorised by the primary impact location on the vehicle. A distinct spatial transition is observed as WAD increases, starting with bumper impacts (blue) concentrated at the lowest WAD values (<1200 mm) and exhibiting a wide range of impact angles, primarily below 50°. As WAD progresses, impacts transition to the hood (green), which represents the most frequent impact zone, with angles predominantly clustered between 75° and 150°. At higher WAD values (>1800 mm), the contact locations shift toward the windshield (brown) and cowl (pink). Notably, the windshield impacts show a downward trend in impact angle as WAD increases, with many points falling below 75° for WAD values exceeding 2000 mm. Roof impacts (purple) are infrequent and occur only at the extreme upper range of the WAD scale.

The evaluation of pedestrian brain injury potential was conducted across multiple simulation modalities, comparing risk predicted by translational (HIC_{15}), rotational (BrIC), and strain-based ($CSDM_{25}$) metrics. For full body simulations (Fig. 7a), head injury risk distributions were highly sensitive to vehicle speed; while HIC_{15} showed a broad range of risks at 30 km/h impact speed, rotational risks (BrIC) and strain risks ($CSDM_{25}$) skewed significantly higher, with BrIC median risks exceeding 0.8 even at lower impact speeds. In contrast, headform simulations (Fig. 7b) and head-only simulations (Fig. 7c) demonstrated a notable decoupling between metrics. In headform-only configurations, HIC_{15} consistently predicted near-maximal injury risk (approaching 1.0) across all impact speed levels, whereas BrIC distributions remained substantially lower and more dispersed, with medians hovering around 0.3. This decoupling occurs because the free-flight headform lacks the neck constraint and torso mass present in full-body impacts, which are the primary biomechanical drivers of the rotational kinematics measured by BrIC. This trend persisted in the head-only simulations, where HIC_{15} maintained a ceiling effect at near-total risk, while $CSDM_{25}$ and BrIC predicted significantly lower injury probabilities. Finally, Fig. 7d shows comparison of head injury risk predicted using the HIC_{15} from headform simulations to the Max Risk representing the highest risk from any individual head injury metric from the full body simulations. The Max Risk correlates well with HIC_{15} from the headform simulations compared to the other individual metric risks.

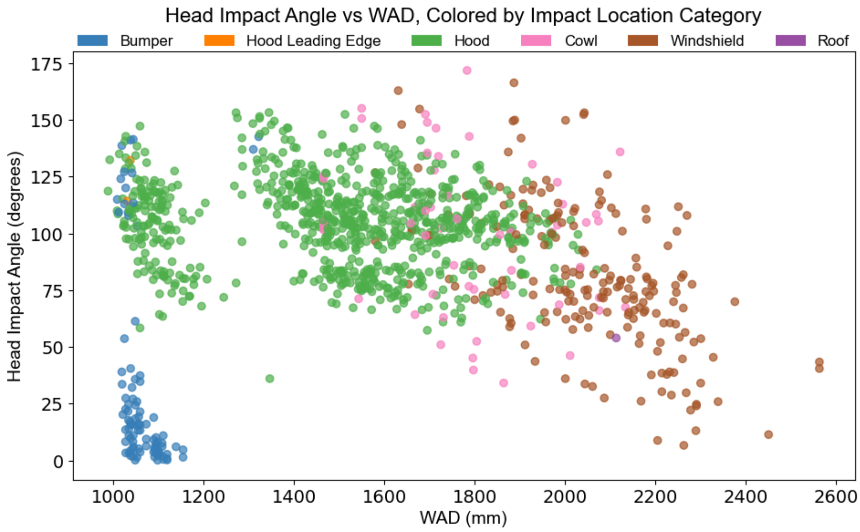

Fig. 6. Distribution of head impact angle vs WAD stratified by impact location.

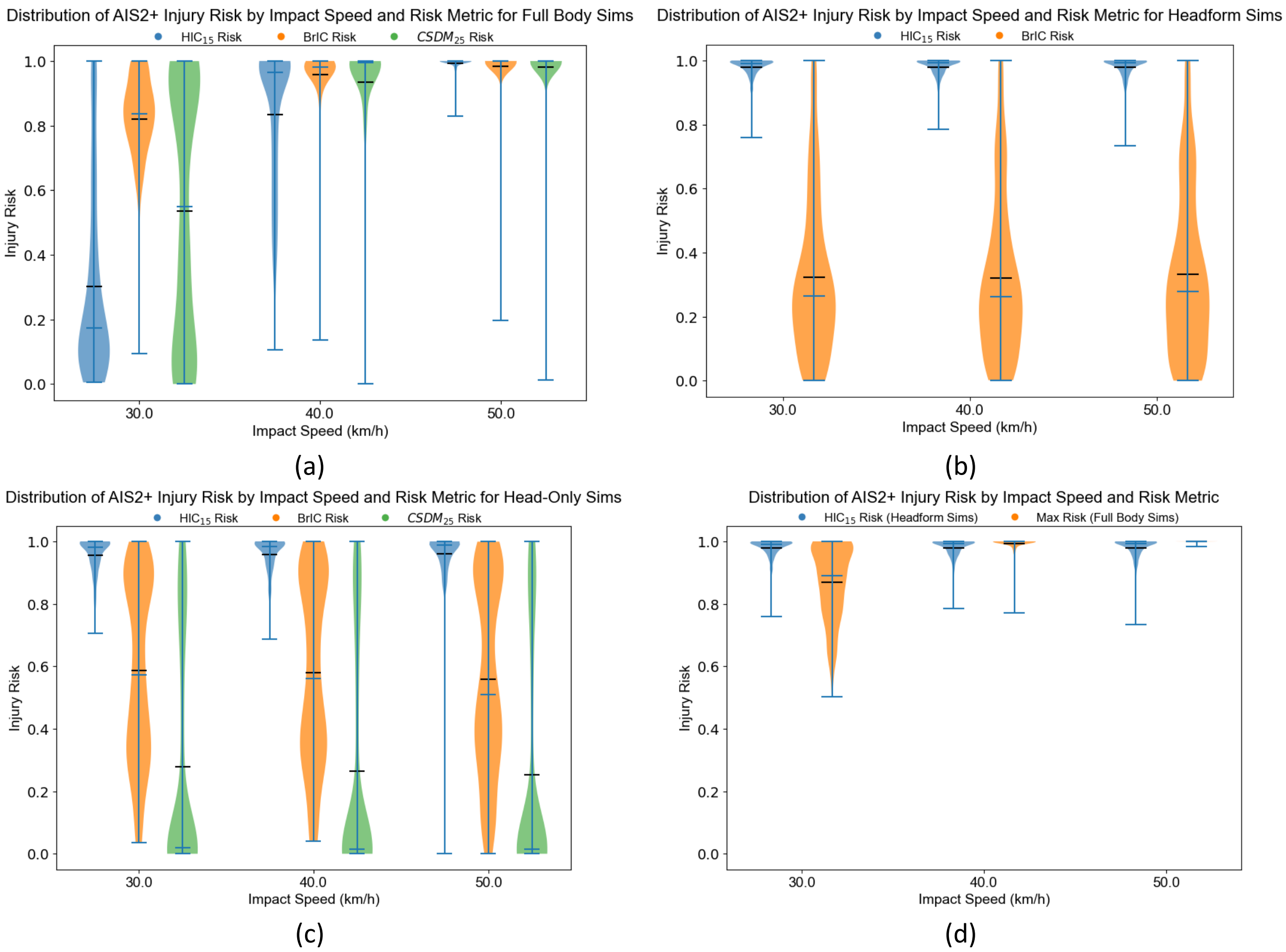

Fig. 7. Distribution of AIS2+ head injury risk based on various metrics grouped by impact speed for full body simulations (a), headform simulations (b), and head-only simulations (c). Comparison of injury risk between headform and full-body simulations (d).

The distribution of AIS2+ head injury risk for full body and headform simulations is reported in TABLE A3. Using a 50% risk threshold to define a positive AIS2+ head injury, the following results compare injury prediction across metrics and modalities. In the full-body simulations (n = 1,152), there were 810, 1,129, and 947 positive injury cases based on HIC_{15}, BrIC, and $CSDM_{25}$, respectively. In contrast, the headform simulations predicted a 100% injury rate (1,152 cases) based on HIC_{15}. Discrepancies between metrics in the full-body simulations highlight the sensitivity of rotational and strain-based measures: HIC_{15} vs. BrIC:

- Only 23 cases showed an injury based on HIC_{15} without a corresponding BrIC injury, whereas 342 cases were positive for BrIC but negative for HIC_{15}.
- HIC_{15} vs. $CSDM_{25}$: Similarly, 37 cases were positive for HIC_{15} only, while 176 cases showed $CSDM_{25}$-based injuries without exceeding the HIC_{15} threshold.
- BrIC vs. $CSDM_{25}$: When comparing the two advanced metrics, 182 cases were positive for BrIC alone, while only two cases were positive for $CSDM_{25}$ without a concurrent BrIC injury.

These results indicate that BrIC is the most conservative metric in full-body kinematics, frequently capturing injury risks that HIC_{15} and $CSDM_{25}$ do not.

IV. Discussion

A large DOE of full body vehicle-to-pedestrian crashes, headform impact, and head-only impact was used to evaluate the pedestrian headform protocol effectiveness. The study used five pedestrian sizes from a 6-years-old child to a 95th percentile male which covers a large population. This was the first study that included a 50th percentile female pedestrian model. The equal allocation of simulations across the five body models was designed to evaluate protocol coverage boundaries for each pedestrian size category, consistent with regulatory DOE methodology, and does not constitute a population-weighted incidence estimate. The 81 vehicle models used in the study cover most of the vehicles sold in the US, from a small sedan to a large truck including minivans. Typically, US vehicles such as SUVs and trucks have taller front ends than vehicles sold in rest of the world, making it important to understand differences in head impact location and patterns. While the standards are not meant to capture all the real-world scenarios, the pedestrian and vehicle models used in the study are representative of the US population and US fleet.

The Euro NCAP uses four zones for headform testing based on WAD values and they are all ahead of the hood leading edge reference line. The first zone is between WAD 1000-1500 mm where a child headform is used, followed by WAD 1500-1700 mm zone that is used for both child and adult headforms, then third and fourth zones between WAD 1700-2100 mm and WAD 2100-2500 mm respectively using the adult headform. The fourth zone was added to account for taller adults and cyclists. These four zones cover the hood, cowl area, windshield, and A-pillars. But proposed FMVSS 228, which is based on GTR 9, uses only two zones, one for the child and adult headforms each. These two zones are between WAD 1000-1700 mm and WAD 1700-2100 mm. Neither FMVSS 228 nor GTR 9 have an overlap zone or region beyond WAD 2100 mm. Both don’t include windshields and A-pillars. Although not part of this study, the cyclist and e-scooter riders had WAD within the range of 2000 – 2500 mm which makes the windshield one of the main sources of head injury [16].

The distribution of the head impacts in Fig. 4 and TABLE A1 shows a considerable number (n=272) of adult head impacts from all four models in the second zone and on the hood, supporting Euro NCAP’s decision of adding this overlap zone. The child headform weight is closer to the F05 head, so use of the child headform for F05 is acceptable but for F50 and above, the adult headform is necessary based on their head mass (TABLE I). Similarly, inclusion of windshields and A-pillars is supported by the fact that all adults had head impact with the windshield (n=204) and extending the testing zones to WAD 2500 will cover taller subjects like M95 (n=80) and in some cases M50 (n=3). Conclusions regarding windshield contact rates are corroborated by independent epidemiological data [11,12] and are not derived solely from simulation incidence proportions.

The headform impact tests are done at 35 km/h as per GTR 9 and FMVSS 228 protocols whereas Euro NCAP protocol uses 40 km/h. There were 685 and 589 cases from the full body simulations where head impact velocity exceeded 35 and 40 km/h respectively, but average head impact velocity was at 39.4 km/h (TABLE A2) which is in line with the Euro NCAP protocol. On the other hand, head impact angle values were considerably higher than the ones that are used in the protocol tests (TABLE A2). All protocols use 65° for the adult headform and 50° for the child headform when the impact location is above 20° and 0° when the impact location is below the hood leading edge reference line. Regardless of the discrepancies in the velocity and angle, headform impact simulations were able to predict AIS 2+ head injury for all cases where full body simulations predicted injury using max risk (TABLE A3). This suggests that the HIC_{15} based risk calculated from the headform test can estimate head injury that covers most of the vehicle-to-pedestrian scenarios if the headform test is carried out as per the Euro NCAP test protocol.

While current regulatory and consumer headform tests provide essential data on vehicle front-end crashworthiness, they fundamentally overlook the "secondary impact" phase, which remains a leading cause of traumatic brain injury. Analysis of real-world accident data from the GIDAS database reveals that over 43% of severe to fatal pedestrian head injuries are attributed to ground contact rather than the initial vehicle strike [17]. While head-to-ground injuries fall outside the scope of current vehicle-pedestrian protocols, they must be understood to effectively reduce total head trauma in vulnerable road users. To address this, safety frameworks are increasingly turning to virtual testing, as seen in the Euro NCAP CP 540, which utilise HBMs to assess full-body kinematics, trajectory, and HIT [15].

Another benefit of adopting virtual testing is the ability to extract injury metrics such as BrIC and $CSDM_{25}$ from HBMs, which are better predictors of brain injury than HIC_{15} [14]. Physical headform testing launches the component at a linear velocity of 40 km/h, completely lacking the rotational components present in real-world vehicle-to-pedestrian crashes. This limitation is effectively resolved by using full-body HBMs in virtual testing.

These advanced simulations are necessary to evaluate the complex synergy between Autonomous Emergency Braking (AEB), which can reduce HIC_{15} values by approximately 50%, and passive countermeasures like active hood lift systems and pedestrian airbags [18]. While integrated systems combining AEB with active hoods and airbags have demonstrated up to 64% effectiveness in reducing severe injuries [18], research indicates that front-end designs optimised for primary impact can inadvertently alter a pedestrian's rotation and pitch, potentially increasing the severity of head-to-ground contact [19]. Therefore, it is imperative for regulatory and consumer bodies to adopt holistic virtual testing to ensure that these interconnected technologies do not achieve vehicle-level HIC_{15} reductions at the expense of landing safety. Ultimately, virtual testing serves as a powerful tool that complements existing physical testing methodologies.

With pedestrian AEB equipped on only ~26% of registered US vehicles as of 2024 and 95% fleet penetration not projected until 2046 [20], passive safety standards retain critical importance. Furthermore, real-world AEB effectiveness is absent at night on unlit road conditions which are associated with 75% of pedestrian fatalities and at speeds exceeding 50 mph [21,22]. The 40 km/h headform test threshold therefore remains relevant as a test condition for residual impact scenarios that AEB cannot fully prevent.

One of the limitations of the study is that the study focused on simulating vehicle-to-pedestrian crashes only at the vehicle centerline which was based on the Euro NCAP CP 540 protocol. In real-world situations, these crashes include a variety of pedestrian postures, impact locations on the vehicles, and directions of impact, which is not captured in this study; however, the design of this study makes it irrelevant as head impact location was consistent between the full body, headform, and head-only simulations. This study used simplified pedestrian and generic vehicle models for computational and cost efficiency for conducting a large number of simulations which is another limitation of the study. However, both these models have been used for similar studies in the past and pedestrian models have been certified to be used for virtual testing.

V. CONCLUSIONS

Results of the study suggest that the Euro NCAP pedestrian protocol headform tests can capture most of the pedestrian-to-vehicle crashes because of its selection of headform impact velocity and four headform impact zones based on WAD. This study demonstrates that the current scope of the proposed FMVSS 228 pedestrian safety regulation which is based on GTR 9 is too narrow to provide comprehensive head protection. The simulation data reveals that stature is a primary determinant of head impact location, with taller adults frequently striking the cowl and windshield, areas currently excluded from the FMVSS 228 and GTR 9 test areas. To align with the evolving international safety landscape and the realities of the US vehicle fleet, the final standard should expand the testable area to WAD 2500, include the windshield as a valid impact location, and increase impact velocity to 40 km/h. Although, HIC_{15} based injury risk from headform tests can accurately estimate head injuries, relying solely on the HIC_{15} metric fails to capture the full spectrum of brain injury risks in full body simulations. For virtual testing with full body human body models, it is recommended to use other injury metrics such as BrIC and $CSDM_{25}$ to accurately estimate head injury.

VI. Acknowledgements

The authors would like to thank the National Highway Traffic Safety Administration for funding this research under grants 693JJ923R000197 and 693JJ921D000024. All simulations were run on the DEMON cluster, a high-performance computing cluster at Wake Forest University School of Medicine, an academic core of Atrium Health Wake Forest Baptist Medical Center, with support from Robert Sutton Jr., and Lenny Shovsky.

VII. Disclosure Statement

F. Scott Gayzik and Joel D. Stitzel are members, and Ashley A. Weaver is a former consultant, of Elemance, LLC., which distributes academic and commercial licenses for the use of GHBMC-owned computational human body models. The opinions, findings, and conclusions expressed in this publication are those of the authors and not necessarily those of the Department of Transportation or the National Highway Traffic Safety Administration.

VIII. References

[1] EuroNCAP. Vulnerable Road User Testing Protocol. 2023, Euro NCAP Secretariat: Brussels, Belgium.

[2] Administration, N.H.T.S. Federal Motor Vehicle Safety Standards; Pedestrian Head Protection. 2024. p. 49 CFR Part 571.

[3] Europe, U.N.E.C.f. Global Technical Regulation No. 9: Pedestrian Safety. 2009, World Forum for Harmonization of Vehicle Regulations (WP.29).

[4] Takhounts, E.G., Craig, M.J., Moorhouse, K., McFadden, J., and Hasija, V. Development of brain injury criteria (BrIC). *Stapp car crash journal*, 2013. 57: p. 243

[5] Gabler, L.F., Crandall, J.R., and Panzer, M.B. Assessment of kinematic brain injury metrics for predicting strain responses in diverse automotive impact conditions. *Annals of biomedical engineering*, 2016. 44(12): p. 3705-3718

[6] Hu, J., Lin, Y.-S., et al. Pedestrian safety: assessment of crashworthiness test procedures. 2023, National Highway Traffic Safety Administration.

[7] Poveda, L., Miller, L.E., et al. Effects of Vehicle Speed, Category, and Front-End Design on Full-Body Injury Risks of a Midsized Male Pedestrian. *SAE International Journal of Transportation Safety*, 2026. 14(1)

[8] Hu, J., Lin, Y.-S., et al. Predicting head impact conditions in vehicle-to-pedestrian impacts through computational human modeling. *Traffic Injury Prevention*, 2025. 26(sup1): p. S181-S189

[9] EuroNCAP. Assessment Protocol - Vulnerable Road User Protection. 2023, Euro NCAP Secretariat: Brussels, Belgium.

[10] Mueller, B.C., Nolan, J.M., Zuby, D.S., and Rizzo, A.G. Pedestrian injury patterns in the United States and relevance to GTR. *Proceedings of Proceedings of IRCOBI conference*, 2012.

[11] Mallory, A., Fredriksson, R., Rosén, E., and Donnelly, B. Pedestrian injuries by source: serious and disabling injuries in US and European cases. *Proceedings of Annals of Advances in Automotive Medicine/Annual Scientific Conference*, 2012.

[12] Fredriksson, R., Rosén, E., and Kullgren, A. Priorities of pedestrian protection--a real-life study of severe injuries and car sources. *Accid Anal Prev*, 2010. 42(6): p. 1672-81

[13] Mueller, B.C. Request for Comments: New Car Assessment Program, Docket No. NHTSA-2023-0020. 2023

[14] Poveda, L., Miller, L.E., et al. Real-world pedestrian crash reconstructions: Vehicle model validation and biomechanical injury analysis. *Traffic Inj Prev*, 2025. 26(sup1): p. S190-S201

[15] EuroNCAP. CP 540 - Pedestrian Human Model Certification. 2025, Euro NCAP Secretariat: Brussels, Belgium.

[16] Van Schijndel, M., De Hair, S., Rodarius, C., and Fredriksson, R. Cyclist kinematics in car impacts reconstructed in simulations and full scale testing with Polar dummy. *Proceedings of 2012 IRCOBI Conference Proceedings-International Research Council on the Biomechanics of Injury*, 2012.

[17] Shang, S., Otte, D., Li, G., and Simms, C. Detailed assessment of pedestrian ground contact injuries observed from in-depth accident data. *Accident Analysis & Prevention*, 2018. 110: p. 9-17

[18] Fredriksson, R. and Rosén, E. Head injury reduction potential of integrated pedestrian protection systems based on accident and experimental data–benefit of combining passive and active systems. *Proceedings of 2014 IRCOBI Conference Proceedings*, 2014.

[19] Gupta, V. and Yang, K.H. Effect of vehicle front end profiles leading to pedestrian secondary head impact to ground. 2013, SAE Technical Paper.

[20] IIHS-HLDI. Predicted availability of safety features on registered vehicles—a 2023 update. *HLDI Bull*, 2023. 40(2)

[21] Cicchino, J.B. Effects of automatic emergency braking systems on pedestrian crash risk. *Accident Analysis & Prevention*, 2022. 172: p. 106686

[22] Sanders, R.L., Schneider, R.J., and Proulx, F.R. Pedestrian fatalities in darkness: What do we know, and what can be done? *Transport policy*, 2022. 120: p. 23-39

IX. APPENDIX

TABLE A1

DISTRIBUTION OF WAD BY IMPACT LOCATION FOR ALL MODELS

Model	Impact Location\WAD	0-1000 mm	1000 – 1500 mm	1500 – 1700 mm	1700 – 2100 mm	2100 – 2500 mm	2500+ mm
6YO	Bumper	-	91	-	-	-	-
	Hood Leading Edge	-	2	-	-	-	-
	Hood	2	148	-	-	-	-
	Cowl	-	-	-	-	-	-
	Windshield	-	-	-	-	-	-
	Roof	-	-	-	-	-	-
F05	Bumper	-	2	-	-	-	-
	Hood Leading Edge	-	-	-	-	-	-
	Hood	-	134	63	4	-	-
	Cowl	-	4	3	2	-	-
	Windshield	-	-	5	3	-	-
	Roof	-	-	-	-	-	-
F50	Bumper	-	-	-	-	-	-
	Hood Leading Edge	-	-	-	-	-	-
	Hood	-	64	122	15	-	-
	Cowl	-	2	3	8	-	-
	Windshield	-	-	5	10	-	-
	Roof	-	-	-	-	-	-
M50	Bumper	-	-	-	-	-	-
	Hood Leading Edge	-	-	-	-	-	-
	Hood	-	-	84	63	-	-
	Cowl	-	-	5	15	-	-
	Windshield	-	-	-	59	3	-
	Roof	-	-	-	-	-	-
M95	Bumper	-	-	-	-	-	-
	Hood Leading Edge	-	-	-	-	-	-
	Hood	-	-	3	94	-	-
	Cowl	-	-	1	15	2	-
	Windshield	-	-	-	41	78	2
	Roof	-	-	-	-	1	-

TABLE A2
SUMMARY STATISTICS FOR HEAD IMPACT VELOCITY AND ANGLE

Model	Head Impact Velocity (km/h)		Head Impact Angle (Degree)	
	Mean	Std	Mean	Std
6YO	30.5	10.6	76.1	45.9
F05	44.4	13.8	102.9	21.9
F50	39.1	11.1	103.1	21.1
M50	39.7	11.0	104.1	26.0
M95	43.7	10.1	87.2	27.4
Adult	41.7	11.8	99.3	25.3
All	39.4	12.4	94.4	32.2

TABLE A3
DISTRIBUTION OF AIS2+ HEAD INJURY RISK

Injury Risk (%)	Full Body Simulations				Headform Simulations
	HIC_{15} Risk	BrIC Risk	$CSDM_{25}$ Risk	Max Risk	HIC_{15} Risk
0 -10	122	2	107	-	-
10-20	87	6	30	-	-
20-30	51	5	17	-	-
30-40	37	5	27	-	-
40-50	45	5	22	-	-
50-60	41	11	19	8	-
60-70	43	37	10	34	-
70-80	40	94	34	70	3
80-90	46	148	67	93	18
90-100	640	839	817	947	1131